npj | science of food

Article

Published in partnership with Beijing Technology and Business University & International Union of Food Science and Technology

https://doi.org/10.1038/s41538-025-00600-x

Luteolin protects against alcoholic liver injury by restoring NRF2 stability to suppress ACSS2 nuclear accumulation

Lixue Cao[1], Qi Lei[1], Yujia Dong[1], Chuyang Meng[1], Qianqian Qi[1], Lisi Li[2], Hongwei Liu[3] ✉, Xifu Liu[1] ✉ & Meng Wang[1,4] ✉

Alcohol abuse results in alcoholic liver disease which are associated with high morbidity and mortality worldwide. Whereas luteolin has shown potential hepatoprotective effects on ethanol-induced liver damage and the underlying mechanism remains unclear. In this study, a chronic plus a single binge ethanol feeding mouse model was employed to mimic acute-on-chronic alcoholic liver injury in humans, and the primary hepatocytes were isolated for the mechanism investigation. Our study demonstrated that luteolin protects against ethanol-induced liver injury by restoring NRF2 stability, thereby blocking the nuclear accumulation of ACSS2 and histone H3 acetylation. This subsequently led to reduced hepatic lipogenesis, and ultimately ameliorated alcoholic liver damage. Our findings elucidate the protective mechanism of luteolin in alcoholic liver injury and provide a new therapeutic strategy for the treatment of alcoholic liver disease.

Liver disease is one leading cause of death accounting for approximately two million deaths annually[1]. Liver injury can be triggered by various factors, including hepatotoxic effectors, viral infections and metabolic disorders, among which, alcohol abuse is a major cause for liver damage[2]. Alcohol is absorbed by small intestine and primarily metabolized by the liver. Alcohol is converted to acetaldehyde, a highly reactive and toxic byproduct in the liver. Under normal conditions, acetaldehyde is rapidly detoxified, however, chronic intake of ethanol causes to the excessive accumulation of toxic acetaldehyde, which possesses the strong oxidizing properties and disrupts liver metabolism and function, contributing to alcohol-induced liver injury. The earliest manifestation of alcohol-related liver damage is alcoholic hepatic steatosis, which is characterized by excessive lipid deposition within hepatocytes. Several factors are associated with hepatic steatosis, including lipid migration and impaired fatty acid β-oxidation[3]. Therefore, inhibiting hepatic lipid deposition represents a promising therapeutic strategy for the treatment of ethanol-induced liver injury.

Cells are constantly exposed to external stressors, including toxic substances, ultraviolet light, and ionizing radiation, which disrupt intracellular metabolic homeostasis[4]. In the context of alcoholic metabolism, ethanol dehydrogenase catalyzes ethanol and convert it to acetaldehyde, a process accompanied by reactive oxygen species (ROS) production. ROS production is one of the main factors that leading to oxidative stress in cells. An elevated ROS level enhances lipid peroxidation of cellular membrane and causes DNA damage, leading to hepatocyte damage[5]. To counteract oxidative stress, organisms have evolved a defense system to protect intracellular homeostasis in response to various oxidative stresses. There are endogenous enzymatic and nonenzymatic antioxidants, which can deplete the excess ROS. As a critical regulator of xenobiotic metabolism, nuclear factor erythroid 2-related factor 2 (NRF2) modulates the expression of genes associated with lipid metabolism, antioxidant response, and mitochondrial biogenesis[6]. Under a homeostatic station, NRF2 binds to kelch-like ECH-associated protein 1 (KEAP1) and exhibits a low transcriptional activity. However, ROS can modify the key cysteine residues in KEAP1, resulting in the accumulation of newly synthesized NRF2. Then, NRF2 translocates to the nucleus and binds to the antioxidant response element (ARE) to promote the antioxidant gene transcription[7].

It is widely recognized that acetyl-CoA synthetase (ACSS) is the main enzyme that condensates acetic acid and coenzyme A to form acetyl-CoA, which is an important intermediate metabolite in energy metabolism[8]. In humans, the ACSS family comprises three isoforms of ACSS1, ACSS2, and

[1]Ministry of Education Key Laboratory of Molecular and Cellular Biology; Hebei Research Center of the Basic Discipline of Cell Biology; Hebei Provincial Technology Innovation Center for Anti-tumor Molecular Targeting New Drugs Development; College of Life Science, Hebei Normal University, Shijiazhuang, China. [2] Department of Biology and Medical Technology, Shijiazhuang Information Engineering Vocational College, Shijiazhuang, Hebei, China. [3] Institute of Biology, Hebei Academy of Sciences, Shijiazhuang, China. [4]State Key Laboratory of New Targets Discovery and Drug Development for Major Diseases, Gannan Innovation and Translational Medicine Research Institute, Gannan Medical University, Ganzhou, China. ✉e-mail: lhwei1987@126.com; xfliu@hebtu.edu.cn; mengwang@hebtu.edu.cn

ACSS3, with distinct substrate preferences and subcellular localizations. ACSS1 and ACSS2 mainly use acetic acid as a substrate[9], while ACSS3 prefers to use propionic acid[10]. Unlike the ACSS1 which exists in mitochondria, ACSS2 is present in cytoplasm and nucleus. ACSS2 shuttles between cytoplasm and nucleus when the external environment changes such as nutrient deficiency or hypoxia[11]. Notably, ACSS2 also plays a key role in the regulation of histone acetylation due to its ability to produce metabolite acetyl-CoA[12]. It was reported that alcohol could induction nuclear accumulation of ACSS2[13,14]. Our previous study also found that ACSS2 was involved in regulating de novo lipogenesis in the liver[14]. These observations strongly suggest that lipid deposition in alcoholic fatty liver may be associated with ACSS2-mediated metabolic and epigenetic alterations.

Previous studies have reported that luteolin, a naturally flavonoid abundantly present in a variety of plants, can regulate physiological functions such as antioxidant, anti-inflammatory, anti-tumor, and inhibition of endoplasmic reticulum stress[15,16]. So far, there are limited reports about luteolin on liver disease, and most study mainly focus on the non-alcoholic fatty liver disease[17,18]. Though the effect of luteolin on alcoholic liver injury was previously reported, the precise molecular mechanisms underlying this protection require further elucidation[19]. In an attempt to gain further insights into the regulation of luteolin on alcoholic liver injury, we employed both the primary hepatocytes and mouse models of alcoholic liver injury. Our work demonstrates that luteolin enhances NRF2 stability, which reduces nuclear accumulation of ACSS2, and ultimately attenuates alcoholic liver damage. These findings not only clarify the hepatoprotective mechanism of luteolin in alcoholic liver injury but also provide a new therapeutic strategy for the treatment of alcoholic liver disease.

Results

Luteolin reduces ethanol-induced hepatic steatosis and improves metabolic dysfunction

Ethanol-induced hepatic steatosis was assessed by biomarkers in plasma and liver firstly. As shown in Fig. 1, luteolin did not affect the body weight of the mice, indicating that luteolin did not exhibit markedly side effects in mice (Fig. 1A). However, ethanol challenge increased the liver to body weight ratio, which was normalized by luteolin (50 mg/kg and 100 mg/kg) treatment (Fig. 1B). Luteolin administration also decreased ethanol-enhanced alanine aminotransferase (ALT), aspartate aminotransferase (AST), and triacylglycerol (TG) levels in plasma (Fig. 1C). H&E staining showed that there was more macrovesicular steatosis in the liver of ethanol-fed mice, but the luteolin treatment group significantly reduced the lipid deposition in the liver (Fig. 1D). In addition, ethanol feeding also caused oxidative stress in the liver. The alteration of ethanol-induced malondialdehyde (MDA), glutathione (GSH), and catalase (CAT) levels was reversed by luteolin supplementation (Fig. 1E). Notably, the alone luteolin administration showed no significant difference compared with the control group in body weight and liver to body weight ratio (Fig. S1A). The H&E staining of pathological sections, including the liver, heart, spleen and kidney, exhibited no significant alterations (Fig. S1B). There was also no marked difference in the plasma ALT, AST, and TG between the control group and the alone luteolin administration group (Fig. S1C). Meanwhile, the hepatic MDA, GSH, and CAT also demonstrated that the alone luteolin administration exhibits no harmful side effects in this liver injury mice model (Fig. S1D). All these results demonstrated that luteolin effectively protects against ethanol-induced liver injury.

Luteolin prevents the nuclear accumulation of ACSS2

Our prior study found that ACSS2 is involved in hepatic lipogenesis[14], so we examined the ACSS2 expression in the mouse liver. Results found that ethanol induction promoted hepatic ACSS2 expression, while luteolin treatment normalized it (Fig. 2A, B). Similar results were found in the primary hepatocytes (Fig. 2C). Exclude the upregulation of nuclear ACSS2, ethanol stimulation also resulted in elevated levels of histone H3 acetylation. Whereas, luteolin reduced histone H3 acetylation (Fig. 2D). Measurement of hepatic lipogenesis-associated genes demonstrated that luteolin significantly protected against ethanol-induced lipogenesis in the liver (Fig. 2E). These results demonstrated that luteolin inhibited the nuclear accumulation of ACSS2, leading to the reduction of lipogenesis in the liver.

Luteolin suppresses oxidative stress by NRF2 activation

Ethanol stimulation leads to oxidative stress[20]. ROS production is a main indicator to reflect the balance between oxidation and antioxidation[21]. As shown in Fig. 3A, ethanol stimulation resulted in increased ROS levels, however, luteolin treatment reduced the ROS content in the liver. NRF2 plays an important role in regulating the antioxidant response. Luteolin treatment decreased the NRF2 protein expression in cytoplasm, but markedly enhanced the expression in nucleus in vivo (Fig. 3B). In addition, luteolin also promoted the antioxidant gene expression of *Ho1*, *Gclc* and *Nqo1* (Fig. 3C). Similar results were found in primary hepatocytes in vitro (Fig. 3D, E).

NRF2 is involved in the nuclear accumulation of ACSS2

Since luteolin prevents the nuclear accumulation of ACSS2, meanwhile, luteolin suppresses oxidative stress by NRF2 activation, we wonder whether oxidative stress accelerates ACSS2 nuclear accumulation. Previous study has shown that H_2O_2 causes oxidative stress[22], while N-acetylcysteine (NAC) is widely known as a strong antioxidant that prevents oxidative stress[23]. Therefore, we employed H_2O_2 to stimulate the primary hepatocytes and measured the ACSS2 nuclear translocation. Results showed that H_2O_2 stimulation increased the ACSS2 expression in nuclear, but both luteolin and the antioxygen NAC (Sigma-Aldrich Shanghai Trading Co., Ltd, Shanghai, China, Cat No.: A9165) downregulated the expression (Fig. 4A), indicating that oxidative stress is associated with the nuclear accumulation of ACSS2. Knocking down of *Nrf2* abolished the alteration effect of luteolin on the nuclear accumulation of ACSS2 (Fig. 4B). Meanwhile, *Nrf2* knockdown also enhanced the histone H3 acetylation compared with the luteolin treatment group (Fig. 4C). After the knockdown of the *Nrf2* gene, the inhibitory effect of luteolin on the hepatic lipogenesis gene was impaired (Fig. 4D). To verify the role of ACSS2 on histone H3 acetylation and hepatic lipogenesis, *Acss2* was knocked down using siRNA in primary hepatocytes. Results showed that *Acss2* knockdown suppressed the histone H3 acetylation and the gene expression of hepatic lipogenesis (Fig. 4E, F). These results suggested that NRF2 was involved in the nuclear accumulation of ACSS2.

Luteolin ameliorates NRF2 stability

Due to the critical role of NRF2 in regulating the nuclear accumulation of ACSS2[24], we examined the role of luteolin on NRF2 expression. As shown in Fig. 5A, luteolin promoted *Nrf2* gene expression, but inhibited *Keap1* gene expression. Meanwhile, luteolin also enhanced the NRF2 protein expression with suppressing the KEAP1 protein expression (Fig. 5B). ROS generated by oxidative stress impairs protein function through oxidative modification, and may impair protein stability through proteasomal degradation[25]. When intracellular protein synthesis was inhibited by cycloheximide, NRF2 was stably expressed from 2 to 24 h. Ethanol stimulation accelerated NRF2 degradation, but the degradation was delayed after luteolin treatment (Fig. 5C). Additionally, ethanol inducted the KEAP1 degradation, while luteolin treatment normalized it (Fig. 5D). These data indicated that ethanol impaired the stability of the NRF2 protein, whereas luteolin protected the abundance of NRF2 protein.

The protective effect of luteolin against alcohol-induced liver injury is attenuated in *Nrf2* knockdown mice

Hepatic *Nrf2* was knocked down using AAV8-*Nrf2* shRNA to confirm the important role of NRF2 in the protective effect of luteolin against alcohol-induced liver injury in mice. After verifying the effectiveness in knockdown mice, the effect of luteolin on ethanol-induced liver injury was assessed. Results exhibited that the hepatic protective effect of luteolin against ethanol was blocked in the hepatic *Nrf2* knockdown mice (Fig. 6A, B). Meanwhile, luteolin significantly prevented the nuclear accumulation of ACSS2, but this

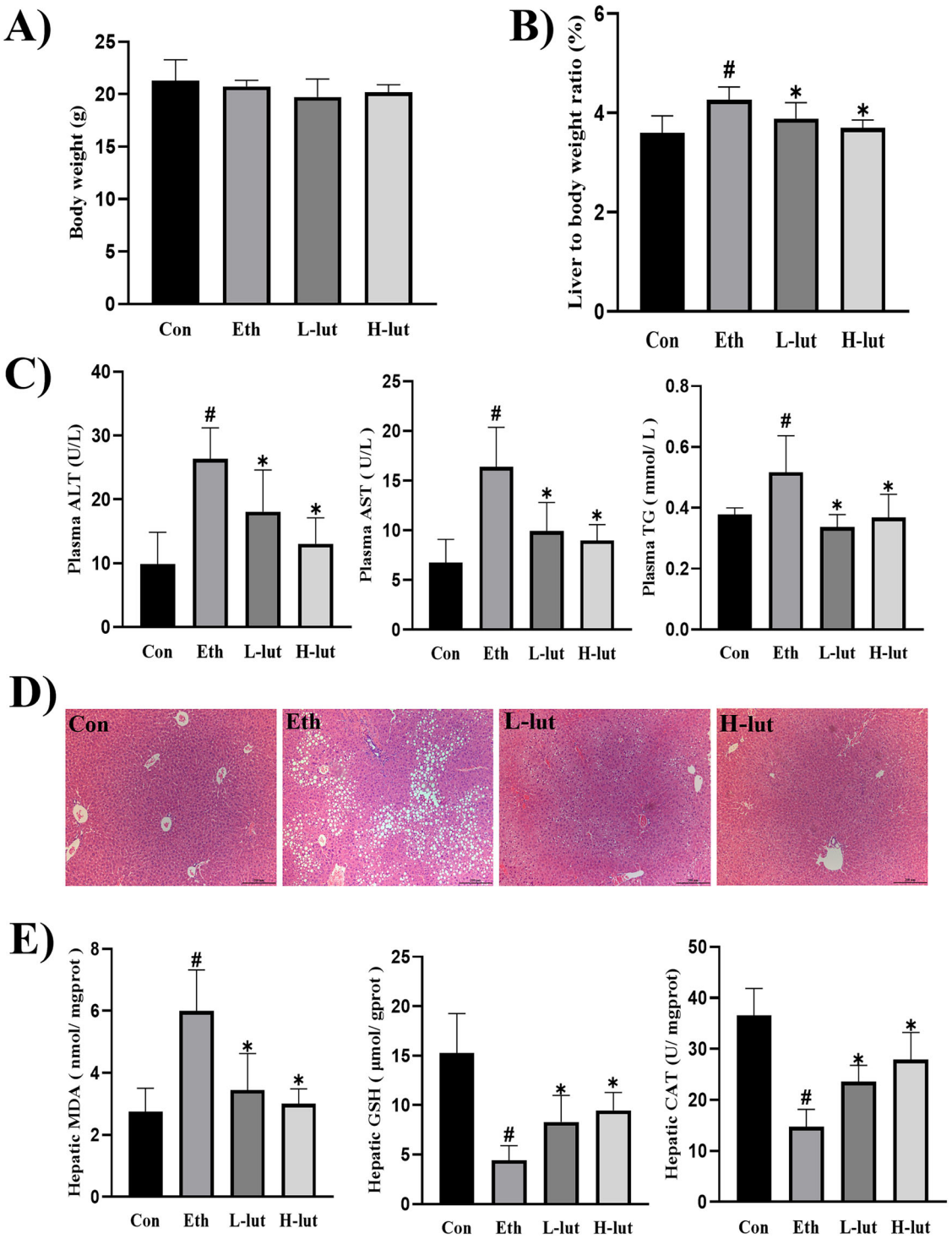

Fig. 1 | Luteolin reduces ethanol-induced hepatic steatosis and improves metabolic dysfunction. A Body weight (n = 8–10). **B** Liver to body weight ratio (n = 8–10). **C** Levels of alanine aminotransferase (ALT), aspartate aminotransferase (AST), and triacylglycerol (TG) in plasma (n = 7–9). **D** The representative hematoxylin and eosin (H&E) staining of liver tissues (×200 magnification) (n = 5, 6). **E** Malondialdehyde (MDA), glutathione (GSH), and catalase (CAT) levels in liver (n = 7–9). Values represent the means ± SD. #$p < 0.05$ vs. Con group; *$p < 0.05$ vs. Eth group. Con control group, Eth ethanol group; L-lut, 50 mg/kg luteolin group; H-lut, 100 mg/kg luteolin group.

effect was counteracted after the knockdown of *Nrf2* in the liver (Fig. 6C). In addition, the effect of luteolin on regulating ethanol-elevated hepatic lipogenesis genes also disappeared (Fig. 6D). These results demonstrated that the protective effect of luteolin on blocking the nuclear accumulation of ACSS2 and thereby inhibiting hepatic lipogenesis to ameliorate liver injury, is dependent on NRF2 activation.

Discussion

Alcoholic liver damage is a progressive disease with high morbidity worldwide[26]. In this study, we found that ethanol-stimulated the nuclear accumulation of ACSS2, which promotes the histone H3 acetylation and accelerates the hepatic lipogenesis gene expression. However, luteolin ameliorated ethanol-induced liver injury by restoring the NRF2 stability to

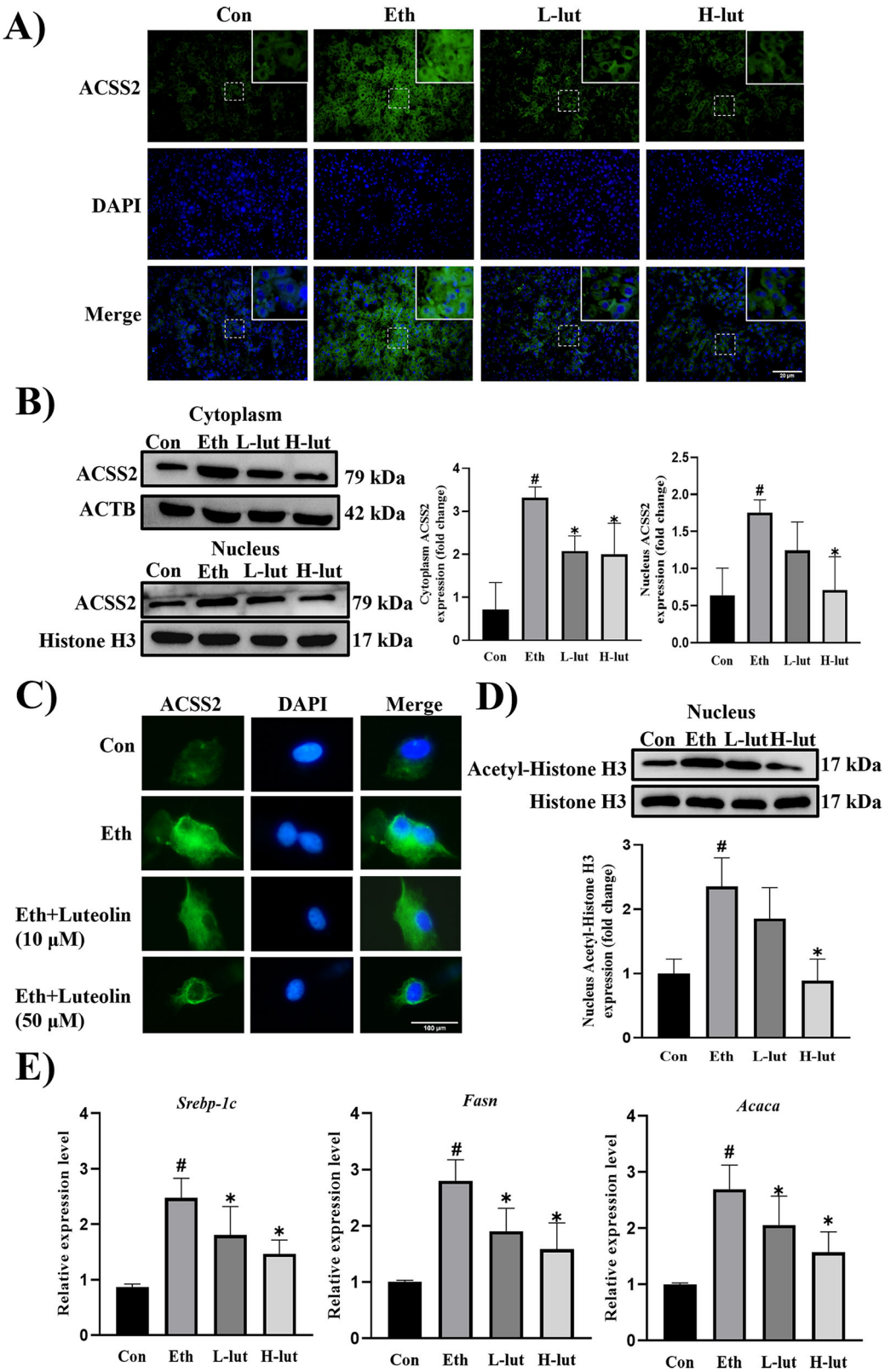

Fig. 2 | Luteolin prevents the nuclear accumulation of ACSS2. **A** Immunofluorescence staining of ACSS2 (green) in liver sections, nucleus was stained with DAPI (blue) (n = 5, 6). **B** Cytoplasm and nucleus protein expression of ACSS2 in liver tissue (n = 4, 5). **C** Immunofluorescence staining of ACSS2 (green) in primary hepatocytes, nucleus was stained with DAPI (blue) (n = 4, 5). **D** Protein expression of acetyl-Histone H3 in liver (n = 4, 5). **E** qPCR analysis of *Srebp-1c*, *Fasn* and *Acaca* genes in liver tissue (n = 6–8). Values represent the means ± SD. #$p < 0.05$ vs. Con group; *$p < 0.05$ vs. Eth group. Con control group, Eth ethanol group; L-lut, 50 mg/kg luteolin group; H-lut, 100 mg/kg luteolin group.

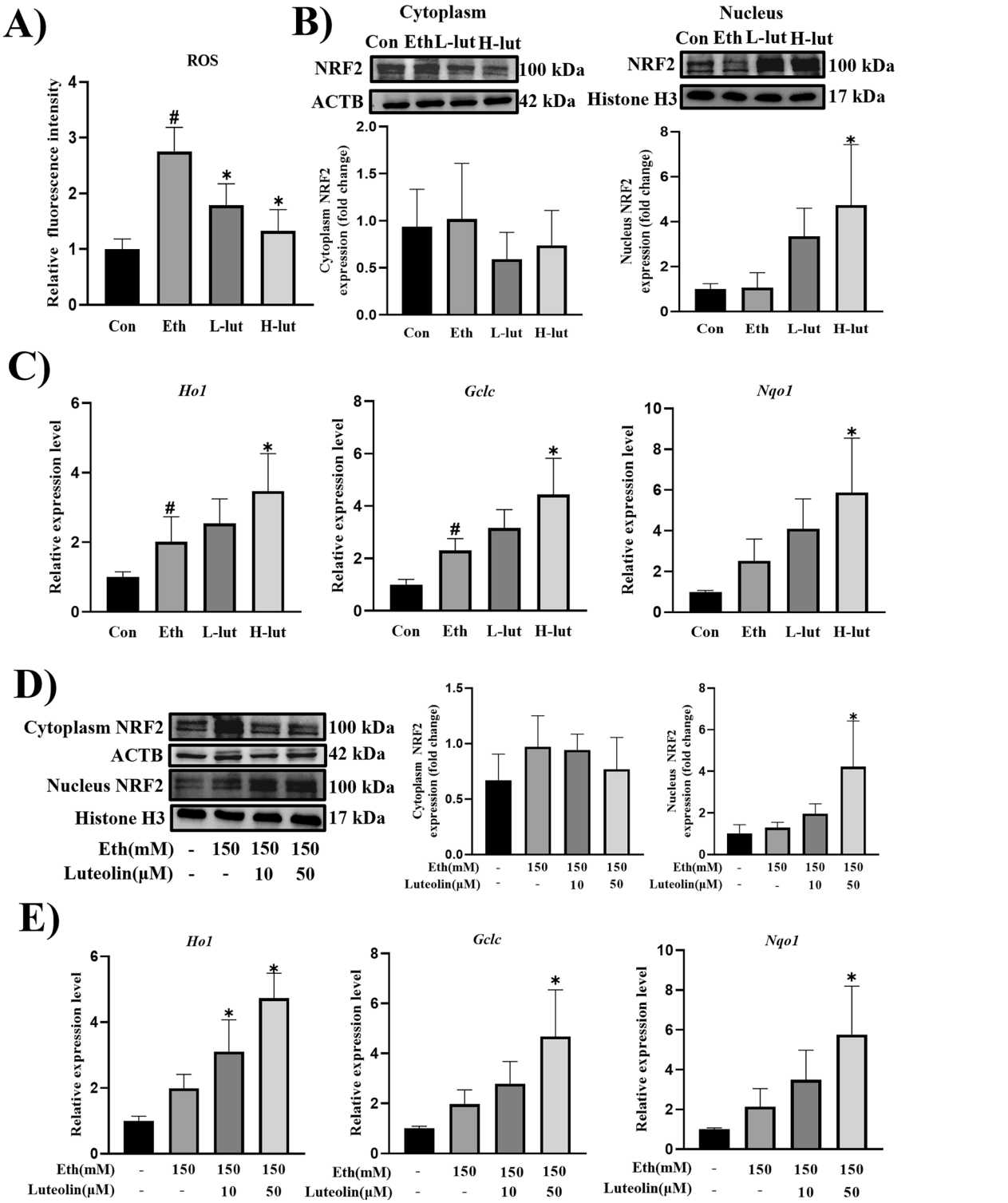

Fig. 3 | Luteolin suppresses oxidative stress by NRF2 activation. **A** Levels of reactive oxygen species (ROS) in liver tissue (n = 7–9). **B** Cytoplasm and nucleus protein expression of NRF2 in liver tissue (n = 4, 5). **C** Genes expression of *Ho1*, *Gclc*, and *Nqo1* in liver tissue (n = 6–8). **D** Cytoplasm and nucleus protein expression of NRF2 in primary hepatocytes (n = 4, 5). **E** Genes expression of *Ho1*, *Gclc*, and *Nqo1* in primary hepatocytes (n = 6–8). Values represent the means ± SD. #$p < 0.05$ vs. Con group; *$p < 0.05$ vs. Eth group. Con control group, Eth ethanol group; L-lut, 50 mg/kg luteolin group; H-lut, 100 mg/kg luteolin group.

prevent ethanol-stimulated nuclear accumulation of ACSS2, contributing to the prevention of alcoholic liver disease (Fig. 7).

Alcoholic liver disease is initially characterized by the transitional accumulation of triglycerides in the liver, which further develops to hepatitis, cirrhosis, and even hepatocellular carcinoma[27,28]. The levels of AST and ALT in plasma are commonly used as biomarkers to reflect liver damage in the clinics. Our study found luteolin significantly downregulated the AST and ALT levels in plasma[29]. Meanwhile, luteolin also suppressed the oxidative stress in alcohol stimulated mice, which is indicated by the hepatic MDA and endogenous antioxidants including the non-enzymatic antioxidants GSH and enzymatic antioxidants CAT. These data demonstrated the hepato-protection effect of luteolin to protect against alcoholic injury in mice.

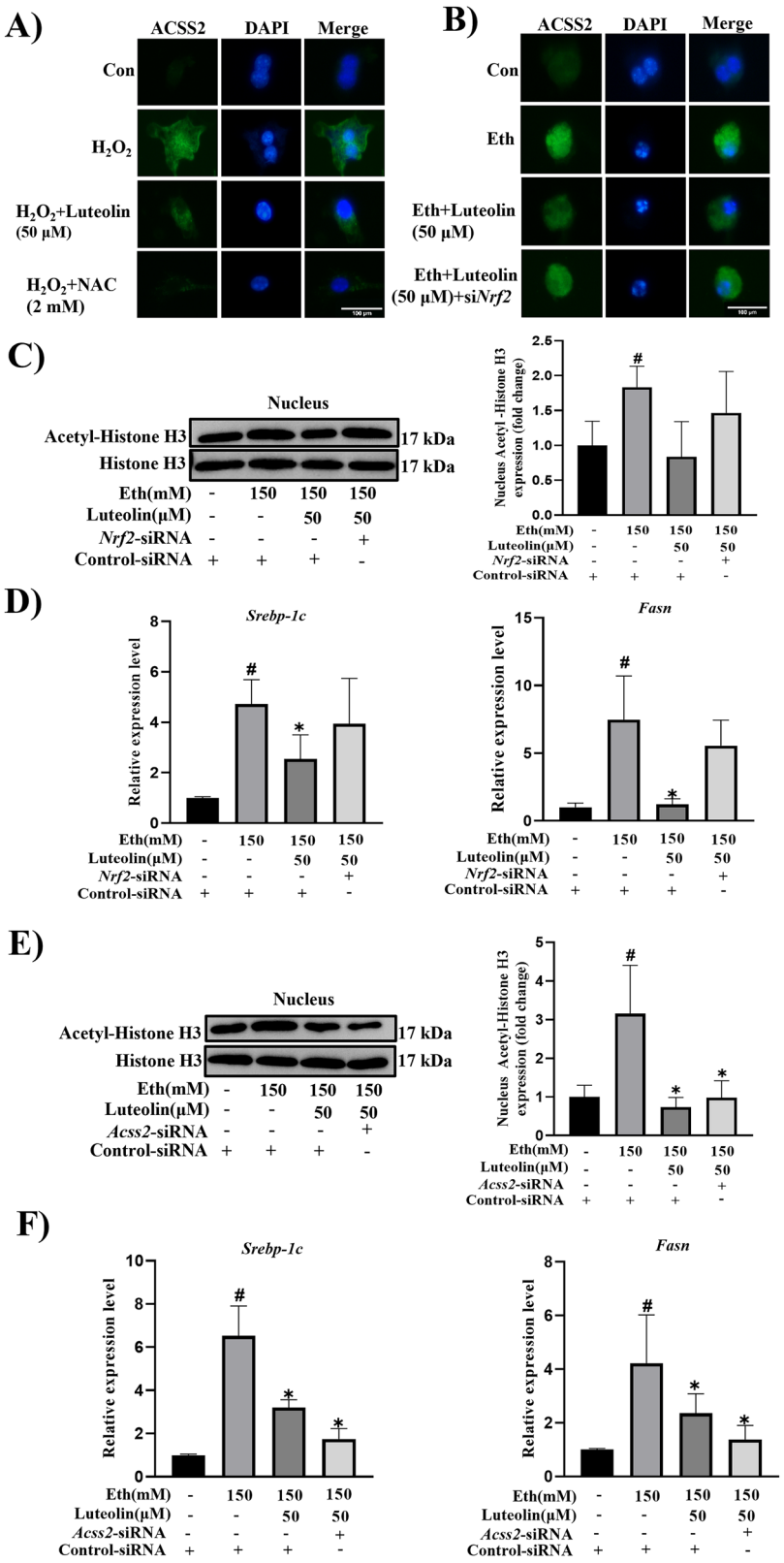

Fig. 4 | NRF2 is involved in the nuclear accumulation of ACSS2. A Representative immunofluorescence staining of ACSS2 (green) after H_2O_2 stimulation in primary hepatocytes, nucleus was stained with DAPI (blue) (n = 4, 5). **B** Representative immunofluorescence staining of ACSS2 (green) after ethanol stimulation in primary hepatocytes, nucleus was stained with DAPI (blue) (n = 4, 5). **C** Protein expression of acetyl-Histone H3 in primary hepatocytes (n = 4, 5). **D** Genes expression of *Srebp-1c* and *Fasn* in primary hepatocytes (n = 6–8). **E** Protein expression of acetyl-Histone H3 in primary hepatocytes (n = 4, 5). **F** Genes expression of *Srebp-1c* and *Fasn* in primary hepatocytes (n = 6–8). Values represent the means ± SD. #$p < 0.05$ vs. Con group; *$p < 0.05$ vs. Eth group. Con control group, Eth ethanol group.

ACSS2, an enzyme that catalyzes the conversion acetic acid to acetyl-CoA, is involved in various metabolic pathways. As is well known, acetic acid is a key intermediate in alcohol metabolism, while acetyl-CoA is a critical substrate for both carbohydrate metabolism and lipid metabolism. Therefore, ACSS2 serves as a central regulator of carbohydrate metabolism and lipid metabolism. Acetic acid is a small molecule that can cross the nuclear pore and produce acetyl-CoA by nuclear ACSS2, which then participate in histone acetylation modification. In addition, ACSS2 can also use the acetic acid generated by the deacetylation reaction in the nucleus to directly and efficiently generate acetyl-CoA in the nucleus, reducing the dependence on extranuclear acetyl-CoA[11]. P Mews et al reported that the metabolism of alcohol drives rapid histone acetylation in the brain, and

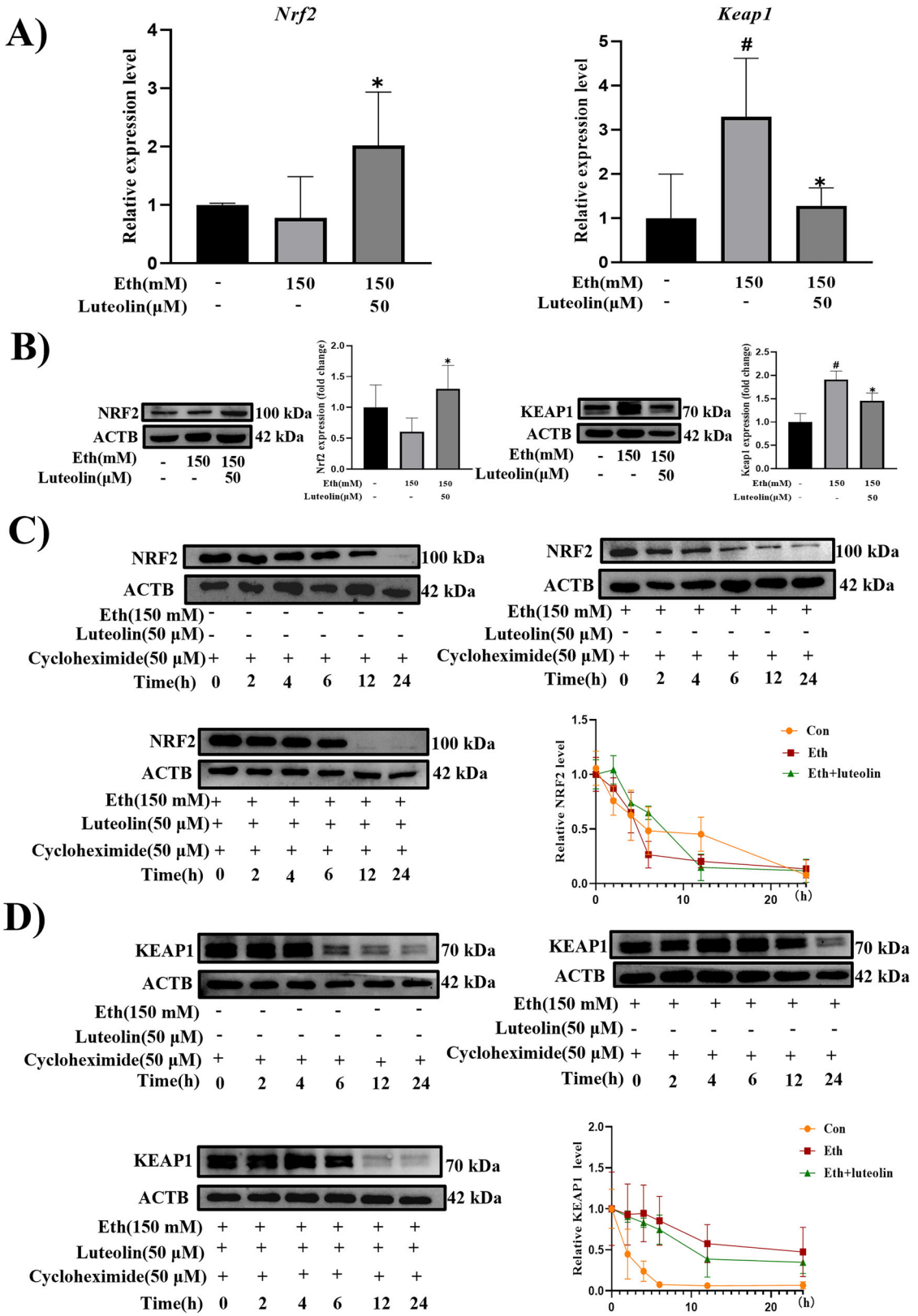

Fig. 5 | Luteolin ameliorates NRF2 stability. A Genes expression of *Nrf2* and *Keap1* in primary hepatocytes (n = 6–8). **B** Protein expression of NRF2 and KEAP1 in primary hepatocytes (n = 4, 5). **C** NRF2 protein degradation in primary hepatocytes (n = 3, 4). **D** KEAP1 protein degradation in primary hepatocytes (n = 3, 4). Values represent the means ± SD. #$p < 0.05$ vs. Con group; *$p < 0.05$ vs. Eth group. Con control group, Eth ethanol group.

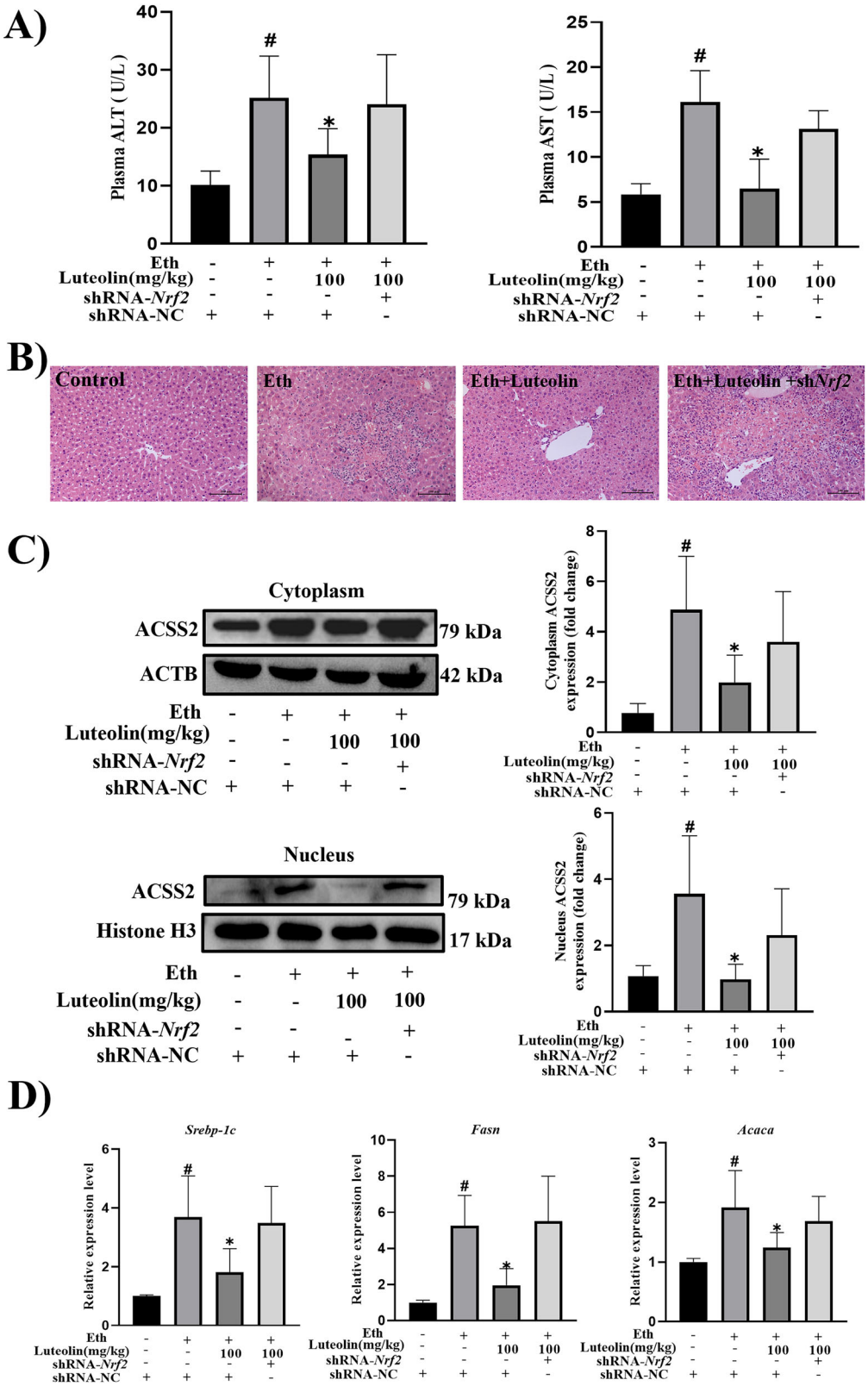

Fig. 6 | The protective effect of luteolin against alcohol-induced liver injury is attenuated in *Nrf2* knockdown mice. **A** Plasma levels of alanine aminotransferase (ALT) and aspartate aminotransferase (AST) in mice (n = 6–8). **B** The representative hematoxylin and eosin (H&E) staining of liver tissues (×200 magnification) (n = 5, 6). **C** Cytoplasm and nucleus expression of ACSS2 protein in liver tissue (n = 4, 5). **D** Genes expression of *Srebp-1c*, *Fasn* and *Acaca* in liver tissue (n = 6–8). Values represent the means ± SD. #$p < 0.05$ vs. Con group; *$p < 0.05$ vs. Eth group. Con control group, Eth ethanol group.

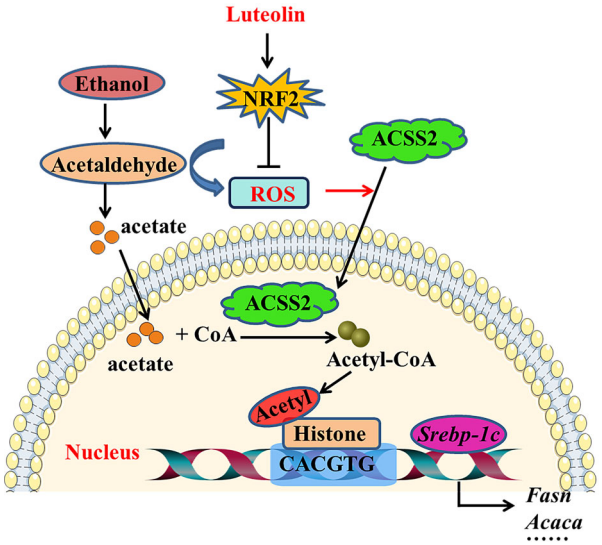

Fig. 7 | Schematic diagram of the potential mechanisms by which luteolin prevents alcoholic liver injury. Alcoholic metabolism progression that ethanol dehydrogenase catalyzes ethanol converting to acetaldehyde, is usually along with reactive oxygen species (ROS) production. ROS promotes the nuclear accumulation of ACSS2, driving the acetyl-CoA production. Acetyl-CoA enhanced the histone H3 acetylation and the expression of hepatic lipogenic genes including *Srebp-1c*, *Fasn* and *Acaca*. Luteolin restored NRF2 stability to suppress the ROS reaction, contributing to the prevention of alcoholic liver disease. *Acaca* acetyl-CoA carboxylase alpha, ACSS2 acetyl-CoA synthetase short-chain family member 2, *Fasn* fatty acid synthase, NRF2 nuclear factor erythroid 2-related factor 2, ROS reactive oxygen species, *Srebp-1c* sterol regulatory element binding transcription factor 1c.

partly through the direct deposition of alcohol-derived acetyl groups onto histones in an ACSS2-dependent manner[13]. Notably, increased nuclear accumulation of ACSS2 has been reported in mice with alcohol-induced liver injury[14]. Consistent with previous results, in the present study, elevated nuclear accumulation of ACSS2 was found in the liver along with the enhanced histone acetylation and lipogenic gene expressions. However, these alterations were reversed by luteolin. These data suggest that luteolin reduces the augmentation of hepatic lipogenesis is, at least partly, associated with blocking the nuclear accumulation of ACSS2.

The chronic plus a single binge ethanol feeding model (NIAAA model) is often used to mimic acute-on-chronic alcoholic liver injury in humans[30]. Prior studies demonstrated that the NIAAA model caused severe hepatic steatosis and liver injury, accompanied by inflammatory responses and oxidative stress[31]. In our research, we found that luteolin reduced ethanol-induced oxidative stress by regulating the NRF2/KEAP1 signaling pathway. NRF2/KEAP1 signaling is widely known as the pathway involved in cellular defense mechanisms against oxidative stress. Activation of the NRF2 system is considered to be a potent cytoprotective strategy. In the physiological state, intracytoplasmic KEAP1 and NRF2 bind, which presents NRF2 for ubiquitination and subsequent degradation by the proteasome[32]. Oxidative stress induces conformational changes, which impair the NRF2 degradation. The protective role of NRF2 in alcohol-induced liver injury has been demonstrated[33,34]. Similarly, our study found that luteolin ameliorated NRF2 stability. Jian Lu et al found that ACSS2 promotes mitochondrial oxidative stress and renal tubular inflammation in diabetic nephropathy[35]. Notably, we found that the nuclear accumulation of ACSS2 is associated with oxidative stress, and knockdown of *Nrf2* markedly prevents the nuclear accumulation of ACSS2.

Taken together, this study provides new insights into the role of luteolin in alcoholic liver injury, which suggests a potential therapeutic strategy to prevent ethanol-induced liver injury.

Methods

Animal treatment

Male C57BL/6 J mice (6–8 weeks) were provided by Liaoning Changsheng Biotechnology Co., Ltd. All mice were housed in an individually ventilated cage (IVC) system with free access to food and water. The room was maintained at 21–25 °C and had 12 h light and dark cycles. In this study, a chronic and binge ethanol feeding mouse model, which is also known as the NIAAA model, was employed to induce the alcoholic liver injury[30]. Briefly, the mice were fed with a modified Lieber-DeCarli liquid diet for 5 days, and after that, all mice were divided into control group, ethanol group, and luteolin treatment groups (50 and 100 mg/kg body weight, Shanghai Aladdin Biochemical Technology Co., Ltd., Shanghai, China, Cat No.: L1267551) randomly. Both the ethanol group mice and the luteolin treatment group mice were fed with an alcohol liquid diet for 10 consecutive days, while the control group mice were fed a control liquid diet equally. All diets were freshly prepared daily for mice and contained 18% protein, 35% fat, 19% carbohydrate, and 28% ethanol or maltodextrin (TROPHIC Animal Feed HighTech Co., Ltd., Nantong, China, Cat No.: TP4030D). For mice luteolin supplementation, luteolin was suspended in sodium carboxymethylcellulose, and then diluted with normal saline (the final concentration of sodium carboxymethylcellulose was 5%). Mice in luteolin-treated groups received luteolin daily by intragastric administration for 10 days consecutively, while the control group mice and the ethanol group mice were orally administered with an equal volume of normal saline with 5% sodium carboxymethylcellulose. On the 11th day, all ethanol-fed mice were gavaged with 31.5% (v/v) ethanol (5 g/kg body weight) in the early morning, while the control group was given the same calorie of maltodextrin. After 9 h of continuous fasting, mice were anesthetized by 2% isoflurane with laparotomy and euthanized with CO_2. The plasma and liver were obtained and stored at −80 °C for subsequent experiments. To assess the side effects of luteolin under physiological conditions, mice in the control group and mice treated with luteolin alone were fed with the control liquid diet for 10 consecutive days. On the 11th day, all mice were orally administered with maltodextrin. After 9 h of continuous fasting, mice were anesthetized by 2% isoflurane with laparotomy and euthanized with CO_2. The plasma, liver, heart, spleen and kidney were collected and stored at −80 °C for subsequent experiments. All animal procedures were operated following the Guidelines for the Care and Use of Laboratory Animals of Hebei Normal University, which was approved by the Animal Ethics Committee of Hebei Normal University (NO.2022LLSC025).

Hepatic specific knocking down of the *Nrf2* gene in mice was obtained using the AAV8-shRNA technique. Meanwhile, the control group mice were injected with AAV8-NC shRNA. After three weeks, *Nrf2* expression in the liver was detected to ensure the effect of AAV8-shRNA. The shRNA sequences used in this experiment were *Nrf2* shRNA: CGAGAAGUGUG UGUGUGACUUUUUUUUA, NC shRNA: TTCTCCGAACGTGT CACGTAA.

Biochemical analysis

Plasma alanine aminotransferase (ALT, Nanjing Jiancheng Bioengineering Institute, Nanjing, China, Cat No.: C009-2-1), aspartate aminotransferase (AST, Nanjing Jiancheng Bioengineering Institute, Nanjing, China, Cat No.: C010-2-1) and triacylglycerol (TG, Nanjing Jiancheng Bioengineering Institute, Nanjing, China, Cat No.: A110-1-1) were measured to reflect liver function. Malondialdehyde (MDA, Nanjing Jiancheng Bioengineering Institute, Nanjing, China, Cat No.: A003-1-1), catalase (CAT, Nanjing Jiancheng Bioengineering Institute, Nanjing, China, Cat No.: A007-1-1) level, and glutathione (GSH, Nanjing Jiancheng Bioengineering Institute, Nanjing, China, Cat No.: A006-2-1) activity in the liver were examined to assess the degree of hepatic oxidative stress. All the experiments were carried out according to the instructions.

Detection of ROS in liver tissue

Freshly taken liver tissues were subjected to tissue homogenization. Hepatocytes were obtained after centrifugation. Then, the cells were incubated

with a DCFH-DA (Beyotime Biotechnology Co., Ltd, Shanghai, China, Cat No.: S0033S) probe for 30 min. The fluorescence intensity of DCFH was detected using a SpectraMax M5 Multi-Mode Microplate Reader (Molecular Devices, CA, USA).

Histological analysis

To evaluate hepatic pathology alteration, the liver was fixed with 4% paraformaldehyde and then embedded in paraffin. The tissue was sliced into 5 μm sections and subjected to hematoxylin and eosin (H&E) (Solarbio Science and Technology Co., Ltd, Beijing, China, Cat No.: G1120) staining. Histopathological alterations were visualized using a Nikon ECLIPSE Ts2 light microscope (Nikon Corporation, Tokyo, Japan).

Primary hepatocytes extraction

Mouse Primary hepatocytes were extracted using a two-step collagenase perfusion method[36,37]. Briefly, mice were anesthetized and the inferior vena cava of the liver was cannulated. The liver was perfused with pre-warmed Hank's Balanced Salt Solution (HBSS, Servicebio Biotechnology Co., Ltd, Wuhan, China, Cat No.: G4203) buffer first. After removing the blood, the buffer was changed to collagenase perfusion. When the liver was enlarged and flaccid, dissect out the liver gently. Subsequently, the liver was minced and continued to be digested in collagenase and shaken for 10 min at 37 °C. HBSS containing 10% FBS (Meilunbio Biotechnology Co., Ltd, Dalian, China, Cat No.: PWL001) was added to terminate the digestion. After being filtered using a 70 μm cell strainer, primary hepatocytes were collected by gradient centrifugation and counted. Finally, primary hepatocytes were plated in dishes and cultured in DMEM (Servicebio Biotechnology Co., Ltd, Wuhan, China, Cat No.: G4524) containing 10% FBS for subsequent experiments.

Immunofluorescence

Primary hepatocytes were plated in 24-well plates and cultured in DMEM with 10% FBS to 80% confluence. After permeabilizing with 0.2% Triton X-100 (Solarbio Science and Technology Co., Ltd, Beijing, China, Cat No.: T8200) for 10 min, the primary hepatocytes were washed with PBS and fixed in 4% paraformaldehyde for 15 min at room temperature. Cells were then blocked with 10% FBS for 1 h at room temperature. Next, the primary hepatocytes were incubated in a humidified cassette with the primary antibody ACSS2 (1:300, Proteintech Group, Inc., Wuhan, China, Cat No.: 16087-1-AP) at 4 °C overnight. The next day, the secondary antibody with fluorescent labeling was incubated at room temperature for 1 h. The nucleus was stained using 4′,6-diamine-2-phenylindole dihydrochloride (DAPI, Biosharp Biotechnology, Hefei, China, Cat No.: BL105A). Fluorescence was observed and photographed by a confocal imaging system (Olympus, Tokyo, Japan). Similarly, the liver tissue was cryosectioned to a thickness of 6 μm. Immunofluorescence of the liver tissue was performed by the same procedure as described above.

Small interfering RNA transfection

To specifically knockdown the *Nrf2* expression, the primary hepatocytes were transfected with specific mouse *Nrf2* or non-silencing control (GenePharma Co., Ltd., Shanghai, China, Cat No.: 112694532) small interfering RNA (siRNA) using Liposome 6000 transfection reagent (Beyotime Biotechnology Co., Ltd, Shanghai, China, Cat No.: C0526). After transfecting the cells for 7 h, the culture medium was changed to DMEM containing 10% FBS. Cells were then used for the subsequent experiments.

Quantitative real-time PCR

Total RNA was extracted from the liver tissue or the primary hepatocytes using the Eastep Super Total RNA extraction kit (Promega Biotechnology Co., Ltd, Beijing, China, Cat No.: LS1040). After measuring its purity, the cDNA was synthesized using HiScript III RT SuperMix for qPCR (Vazyme Biotech Co., Ltd, Nanjing, China, Cat. No.: R323-01) according to the instructions. All gene expressions were quantified using the ChamQ Universal SYBR qPCR Master Mix Kit (Vazyme Biotech Co., Ltd, Nanjing, China, Cat No.: Q311-02/03) on a QuantStudio5 system (Thermo Fisher Scientific Inc., MA, USA). The results were calculated by normalizing the expression of the internal reference *Actb* and setting the control group as one. Primers were designed from the PrimerBank (http://pga.mgh.harvard.edu/primerbank) and synthesized by Sangon (Sangon Biological Engineering Technology & Services Co., Ltd, Shanghai, China). The primer sequences used in this study are shown in Table 1.

Immunoblot analysis

Both nucleus and cytoplasm proteins were extracted from liver tissue or cells using a lysate containing 1% Phenylmethanesulfonyl fluoride (PMSF,

Table 1 | Primer sequence for qRT-PCR

Gene	NCBI Reference Sequence	Gene ID	Primer sequence (5′-3′)
Srebp-1c	NM_001358314.1	20787	Forward: TGACCCGGCTATTCCGTGA
			Reverse: CTGGGCTGAGCAATACAGTTC
Fasn	NM_007988.3	14104	Forward: AGGTGGACTGGATACACAGAC
			Reverse: TCTCCTGCCCAAACTCTTTGC
Acaca	NM_133360.3	107476	Forward: GATGAACCATCTCCGTTGGC
			Reverse: GACCCAATTATGAATCGGGAGTG
Ho1	NM_010442.2	15368	Forward: AAGCCGAGAATGCTGAGTTCA
			Reverse: GCCGTGTAATATGGTACAAGGA
Nqo1	NM_008706.5	18104	Forward: AGGATGGGAGGTACTCGAATC
			Reverse: AGGCGTCCTTCCTTATATGCTA
Gclc	NM_010295.2	14629	Forward: GGGGTGACGAGGTGGAGTA
			Reverse: GTTGGGGTTTGTCCTCTCCC
Nrf2	NM_010902.5	18024	Forward: TCTTGGAGTAAGTCGAGAAGTGT
			Reverse: GTTGAAACTGAGCGAAAAAGGC
Keap1	NM_016679.4	50868	Forward: TGCCCCTGTGGTCAAAGTG
			Reverse: GGTTCGGTTACCGTCCTGC
Actb	NM_007393.5	11461	Forward: GGCTGTATTCCCCTCCATCG
			Reverse: CCAGTTGGTAACAATGCCATGT

Solarbio Science and Technology Co., Ltd, Beijing, China, Cat No.: P8340) and 1% cocktail (Solarbio Science and Technology Co., Ltd, Beijing, China, Cat No.: IKM1010). Proteins were separated using 10% SDS-PAGE and later transferred to a PVDF membrane (Sigma-Aldrich Shanghai Trading Co., Ltd, Shanghai, China, Cat No.: IPVH00010). After blocking with 5% skimmed milk at room temperature for 1 h, the membrane was incubated with the primary antibodies including anti-ACSS2 (79 kDa, 1:3000, Proteintech Group, Inc., Wuhan, China, Cat No.: 16087-1-AP), anti-Histone H3 (17 kDa, 1:1000, Proteintech Group, Inc., Wuhan, China, Cat No.: 17168-1-AP), anti-Acetyl-Histone H3 (17 kDa, 1:1000, Cell Signaling Technology, Inc., Danvers, MA, USA, Cat No.: 8173 T), anti-NRF2 (100 kDa, 1;1000, Cell Signaling Technology, Inc., Danvers, MA, USA, Cat No.: 12721 T), anti-KEAP1 (70 kDa, 1:3000, Proteintech Group, Inc., Wuhan, China, Cat No.: 10503-2-AP) and anti-ACTB (42 kDa, 1:1000, Cell Signaling Technology, Inc., Danvers, MA, USA, Cat No.: 4967S) at 4 °C overnight. The next day, membranes were washed with TBST and incubated with the horseradish peroxidase (HRP)-conjugated goat anti-rabbit IgG antibody (1:10,000, Abcam, Cambridge, MA, USA, Cat No.: ab6721) for 1 h at room temperature. Chemiluminescent detection was performed with ClarityTM Westen ECL Substrate (BioRad Laboratories, Inc., Hercules, CA, USA, Cat No.:1705061) on a Bio-Rad ChemiDoTM XRS System (BioRad Laboratories, Inc., Hercules, CA, USA). Greyscale values were counted by Image J software.

Statistical analysis

All data were expressed as mean ± standard deviation (SD). The results were analyzed using one-way analysis of variance (ANOVA) with Tukey's post hoc test. $p < 0.05$ was considered as statistically significant difference. GraphPad Prism 7.00 software (San Diego, CA, USA) was used for statistical analyses and graphing.

Data availability

The data that support the findings of this study are available from the corresponding author upon reasonable request.

Received: 21 May 2025; Accepted: 2 October 2025;
Published online: 17 November 2025

References

1. Devarbhavi, H. et al. Global burden of liver disease: 2023 update. *J. Hepatol.* **79**, 516–537 (2023).
2. Meza, V. et al. Alcohol consumption: medical implications, the liver and beyond. *Alcohol Alcohol* **57**, 283–291 (2022).
3. Gao, B. & Bataller, R. Alcoholic liver disease: pathogenesis and new therapeutic targets. *Gastroenterology* **141**, 1572–1585 (2011).
4. Ulasov, A. V. et al. Nrf2/Keap1/ARE signaling: towards specific regulation. *Life Sci.* **291**, 120111 (2022).
5. Leung, T. M. & Nieto, N. CYP2E1 and oxidant stress in alcoholic and non-alcoholic fatty liver disease. *J. Hepatol.* **58**, 395–398 (2013).
6. Morgenstern, C. et al. Biomarkers of NRF2 signalling: current status and future challenges. *Redox Biol.* **72**, 103134 (2024).
7. Hayes, J. D. & Dinkova-Kostova, A. T. The Nrf2 regulatory network provides an interface between redox and intermediary metabolism. *Trends Biochem. Sci.* **39**, 199–218 (2014).
8. Yun, M. et al. The importance of acetyl coenzyme A synthetase for 11C-acetate uptake and cell survival in hepatocellular carcinoma. *J. Nucl. Med.* **50**, 1222–1228 (2009).
9. Gao, X. et al. Acetate functions as an epigenetic metabolite to promote lipid synthesis under hypoxia. *Nat. Commun.* **7**, 11960 (2016).
10. Zhou, L. et al. ACSS3 represses prostate cancer progression through downregulating lipid droplet-associated protein PLIN3. *Theranostics* **11**, 841–860 (2021).
11. Bulusu, V. et al. Acetate recapturing by nuclear acetyl-CoA synthetase 2 prevents loss of histone acetylation during oxygen and serum limitation. *Cell Rep.* **18**, 647–658 (2017).
12. Moffett, J. R. et al. Acetate revisited: a key biomolecule at the nexus of metabolism, epigenetics and oncogenesis-part 1: acetyl-CoA, acetogenesis and acyl-CoA short-chain synthetases. *Front. Physiol.* **11**, 580167 (2020).
13. Mews, P. et al. Alcohol metabolism contributes to brain histone acetylation. *Nature* **574**, 717–721 (2019).
14. Lu, Y. et al. Inhibition of ACSS2 attenuates alcoholic liver steatosis via epigenetically regulating de novo lipogenesis. *Liver Int.* **43**, 1729–1740 (2023).
15. Huang, L. et al. Immunopharmacological activities of luteolin in chronic diseases. *Int. J. Mol. Sci.* **24**, 2136 (2023).
16. Kou, J. J. et al. Luteolin alleviates cognitive impairment in Alzheimer's disease mouse model via inhibiting endoplasmic reticulum stress-dependent neuroinflammation. *Acta Pharmacol. Sin.* **43**, 840–849 (2022).
17. Guo, W. et al. Luteolin alleviates methionine-choline-deficient diet-induced non-alcoholic steatohepatitis by modulating host serum metabolome and gut microbiome. *Front. Nutr.* **9**, 936237 (2022).
18. Liu, X. et al. Luteolin alleviates non-alcoholic fatty liver disease in rats via restoration of intestinal mucosal barrier damage and microbiota imbalance involving in gut-liver axis. *Arch. Biochem. Biophys.* **711**, 109019 (2021).
19. Liu, G. et al. Luteolin alleviates alcoholic liver disease induced by chronic and binge ethanol feeding in mice. *J. Nutr.* **144**, 1009–1015 (2014).
20. Koch, O. R. et al. Oxidative stress and antioxidant defenses in ethanol-induced cell injury. *Mol. Asp. Med.* **25**, 191–198 (2004).
21. Schieber, M. & Chandel, N. S. ROS function in redox signaling and oxidative stress. *Curr. Biol.* **24**, R453–R462 (2014).
22. Sies, H. Hydrogen peroxide as a central redox signaling molecule in physiological oxidative stress: oxidative eustress. *Redox Biol.* **11**, 613–619 (2017).
23. Pedre, B. et al. The mechanism of action of N-acetylcysteine (NAC): the emerging role of H2S and sulfane sulfur species. *Pharmacol. Ther.* **228**, 107916 (2021).
24. Odera, J. O. et al. NRF2/ACSS2 axis mediates the metabolic effect of alcohol drinking on esophageal squamous cell carcinoma. *Biochem. J.* **477**, 3075–3089 (2020).
25. Raynes, R., Pomatto, L. C. & Davies, K. J. Degradation of oxidized proteins by the proteasome: distinguishing between the 20S, 26S, and immunoproteasome proteolytic pathways. *Mol. Asp. Med.* **50**, 41–55 (2016).
26. Rehm, J. et al. Global burden of disease and injury and economic cost attributable to alcohol use and alcohol-use disorders. *Lancet* **373**, 2223–2233 (2009).
27. Jeon, S. & Carr, R. Alcohol effects on hepatic lipid metabolism. *J. Lipid Res.* **61**, 470–479 (2020).
28. Altamirano, J. & Bataller, R. Alcoholic liver disease: pathogenesis and new targets for therapy. *Nat. Rev. Gastroenterol. Hepatol.* **8**, 491–501 (2011).
29. Sheth, S. G. et al. AST/ALT ratio predicts cirrhosis in patients with chronic hepatitis C virus infection. *Am. J. Gastroenterol.* **93**, 44–48 (1998).
30. Bertola, A. et al. Mouse model of chronic and binge ethanol feeding (the NIAAA model). *Nat. Protoc.* **8**, 627–637 (2013).
31. Dong, M. et al. Mangiferin protects against alcoholic liver injury via suppression of inflammation-induced adipose hyperlipolysis. *Food Funct.* **11**, 8837–8851 (2020).
32. Itoh, K. et al. Keap1 represses nuclear activation of antioxidant responsive elements by Nrf2 through binding to the amino-terminal Neh2 domain. *Genes Dev.* **13**, 76–86 (1999).
33. Nagappan, A., Kim, J. H., Jung, D. Y. & Jung, M. H. Cryptotanshinone from the salvia miltiorrhiza bunge attenuates ethanol-induced liver injury by activation of AMPK/SIRT1 and Nrf2 signaling pathways. *Int. J. Mol. Sci.* **21**, 265 (2019).

34. Wang, X. et al. Curcumin and Baicalin ameliorate ethanol-induced liver oxidative damage via the Nrf2/HO-1 pathway. *J. Food Biochem.* **44**, e13425 (2020).
35. Lu, J. et al. Acetyl-CoA synthetase 2 promotes diabetic renal tubular injury in mice by rewiring fatty acid metabolism through SIRT1/ChREBP pathway. *Acta Pharmacol. Sin.* **45**, 366–377 (2024).
36. Mendoza, R. et al. Isolation and culture of mouse hepatocytes and kupffer cells (KCs). *Methods Mol. Biol.* **2455**, 73–84 (2022).
37. Charni-Natan, M. & Goldstein, I. Protocol for primary mouse hepatocyte isolation. *STAR Protoc.* **1**, 100086 (2020).

Acknowledgements

This work was supported by the Natural Science Foundation of Hebei Province (grant number H2022205007) and Science Foundation of Hebei Normal University (grant numbers L2024K03) and High-level talents training and funding projects of Hebei academy of sciences (2024G11) and open research (Subject No. SKLD2024Q02) fund of State Key Laboratory of New Targets and Drug Development for Major Diseases. Special thanks to Prof. Sanbing Shen from National University of Ireland for his contribution in improving the language.

Author contributions

Conceptualization: M.W. X.F.L. and H.W.L.: Conceived the study and wrote the original draft. L.X.C. and Q.L.: Operated the experiments. Y.J.D. and C.Y.M.: Performed and analyzed the data. Q.Q.Q. and L.S.L.: Revised the manuscript.

Competing interests

The authors declare no competing interests.

Additional information

Supplementary information The online version contains supplementary material available at https://doi.org/10.1038/s41538-025-00600-x.

Correspondence and requests for materials should be addressed to Hongwei Liu, Xifu Liu or Meng Wang.